

Article

Phase Behavior of Carbon Dioxide + Isobutanol and Carbon Dioxide + *tert*-Butanol Binary Systems

Sergiu Sima¹, Adrian Victor Crişciu^{1,*} and Catinca Secuianu^{1,2,*} 

¹ Department of Inorganic Chemistry, Physical Chemistry and Electrochemistry, Faculty of Applied Chemistry and Materials Science, University “Politehnica” of Bucharest, 1-7 Gh. Polizu Street, S1, 011061 Bucharest, Romania; sergiu.sima@upb.ro

² Department of Chemical Engineering, Imperial College London, South Kensington Campus, London SW7 2AZ, UK

* Correspondence: adrian.crisciu@upb.ro (A.V.C.); catinca.secuianu@upb.ro or c.secuianu@imperial.ac.uk (C.S.); Tel.: +40-21-4023823 (C.S.)

Abstract: In recent years, the dramatic increase of greenhouse gases concentration in atmosphere, especially of carbon dioxide, determined many researchers to investigate new mitigation options. Thermodynamic studies play an important role in the development of new technologies for reducing the carbon levels. In this context, our group investigated the phase behavior (vapor–liquid equilibrium (VLE), vapor–liquid–liquid equilibrium (VLLE), liquid–liquid equilibrium (LLE), upper critical endpoints (UCEPs), critical curves) of binary and ternary systems containing organic substances with different functional groups to determine their ability to dissolve carbon dioxide. This study presents our results for the phase behavior of carbon dioxide + *n*-butanol structural isomers binary systems at high-pressures. Liquid–vapor critical curves are measured for carbon dioxide + isobutanol and carbon dioxide + *tert*-butanol binary systems at pressures up to 147.3 bar, as only few scattered critical points are available in the literature. New isothermal vapor–liquid equilibrium data are also reported at 363.15 and 373.15 K. New VLE data at higher temperature are necessary, as only another group reported some data for the carbon dioxide + isobutanol system, but with high errors. Phase behavior experiments were performed in a high-pressure two opposite sapphire windows cell with variable volume, using a static-analytical method with phases sampling by rapid online sample injectors (ROLSI) coupled to a gas chromatograph (GC) for phases analysis. The measurement results of this study are compared with the literature data when available. The new and all available literature data for the carbon dioxide + isobutanol and carbon dioxide + *tert*-butanol binary systems are successfully modeled with three cubic equations of state, namely, General Equation of State (GEOS), Soave–Redlich–Kwong (SRK), and Peng–Robinson (PR), coupled with classical van der Waals mixing rules (two-parameter conventional mixing rules, 2PCMR), using a predictive method.

Keywords: phase behavior; critical curve; carbon dioxide; isobutanol; *tert*-butanol; EoS; high-pressures



Citation: Sima, S.; Crişciu, A.V.; Secuianu, C. Phase Behavior of Carbon Dioxide + Isobutanol and Carbon Dioxide + *tert*-Butanol Binary Systems. *Energies* **2022**, *15*, 2625. <https://doi.org/10.3390/en15072625>

Academic Editors: Yolanda Sanchez Vicente, J. P. Martin Trusler and Saif Al Ghafri

Received: 4 March 2022

Accepted: 29 March 2022

Published: 3 April 2022

Publisher’s Note: MDPI stays neutral with regard to jurisdictional claims in published maps and institutional affiliations.



Copyright: © 2022 by the authors. Licensee MDPI, Basel, Switzerland. This article is an open access article distributed under the terms and conditions of the Creative Commons Attribution (CC BY) license (<https://creativecommons.org/licenses/by/4.0/>).

1. Introduction

The constant increase of greenhouse gases in the atmosphere and consequently climate change determined researchers to search for new mitigation options [1–4]. At the same time, the knowledge of phase behavior and thermophysical properties is a critical pre-requisite for optimal design and operation in a variety of industrial applications involving pure components and mixtures [2,4]. In this context, we focused lately on the study of phase behavior of mixtures containing carbon dioxide and organic substances with different functional groups [5–8]. For instance, we studied binary systems of carbon dioxide and three different oxygenated organic compounds with four carbon atoms, specifically ethyl acetate (ester), 1,4-dioxane (cyclic ether), and 1,2-dimethoxyethane (linear diether) [5]. While the two first compounds are structural isomers with the formula C₄H₈O₂, the last one is a linear diether with the formula C₄H₁₀O₂. Our study revealed that the CO₂ solubility

increases in the order 1,4-dioxane < ethyl acetate < 1,4-dimethoxyethane which means that ethers are better solvents than esters, but oxygenated cyclic compounds have the lowest performance.

Today more than never, it is important to find alternative sources of energy, and as fossil fuels will continue to be the primary source of energy in the next years due to several factors (availability, price, ease of transportation, other), finding a suitable candidate for CO₂ capture and/or applications in the field of CCS and CCUS technologies remains one of the key topics. Research and development of highly effective CO₂ separation and capture technologies are still required to meet CO₂ reduction targets [1]. Therefore, the fundamental understanding of the phase behavior as well as the possible applications, especially new carbon mitigation ways, are the main motivations of our study. Among the organic species chosen as the second component in the study of the equilibrium between phases at high pressures in binary systems containing carbon dioxide, alcohols occupy an important place, due their multiple uses [9,10]. In addition, the carbon dioxide + *n*-alcohols series is one of the few for which the types of fluid phase diagram, according to the classification of van Konyneburg and Scott [11,12], are known [13–15]. While the global phase behavior is elucidated for carbon dioxide + *n*-alcohols, the carbon dioxide + branched alcohols received less attention, and for most systems, only vapor–liquid equilibria (VLE) in a limited range of temperatures and pressures are reported [2,16–20]. Thus, the phase behavior of both carbon dioxide + 1-butanol and + 2-butanol, its chain isomer, and binary systems are attributed to type II phase behavior. The carbon dioxide + isobutanol binary system belongs to type II phase behavior [21], while the carbon dioxide + *tert*-butanol system can be attributed to type I or II phase behavior [22]. Both types are characterized by a continuous liquid–vapor critical curve stretching between the critical points of pure components. The difference between type I and type II phase behavior is that the latter presents an additional liquid–liquid (LL) critical locus which intersects a three-phases liquid–liquid–vapor equilibrium (LLVE) curve in an upper critical endpoint (UCEP) (Table 1).

Table 1. Literature ^a VLE experimental data for carbon dioxide + isobutanol and + *tert*-butanol.

<i>P</i> or <i>P</i> _{range} /bar	<i>T</i> or <i>T</i> _{range} /K	<i>N</i> _{exp}	Observations	Ref.
carbon dioxide (1) + isobutanol (2)				
18.26 ÷ 81.40	313.15	10	<i>P</i> - <i>x</i>	[23]
17.30 ÷ 130.0	333.15 ÷ 353.15	23	<i>P</i> - <i>x,y</i>	[21]
carbon dioxide (1) + <i>tert</i> -butanol (2)				
70.0 ÷ 115.2	333 ÷ 368	14	<i>P</i> - <i>x</i>	[24]
103.5 ÷ 120.3	343 ÷ 368	6	<i>P</i> - <i>y</i>	
19.5 ÷ 112.9	323.15 ÷ 353.15	30	<i>P</i> - <i>x,y</i>	[22]
10.3 ÷ 75.5	313.15	13	<i>P</i> - <i>x</i>	[25]
14.5 ÷ 79.16	313.15	10	<i>P</i> - <i>x</i>	[23]

^a Not considered in our previous studies [21,22].

Previously, we reported isothermal vapor–liquid equilibrium data at 333.15, 343.15, and 353.15 K for carbon dioxide + isobutanol binary system [21] and at 323.15, 333.15, 343.15, and 353.15 K for the carbon dioxide + *tert*-butanol system [22]. Isobutanol (2-methyl-1-propanol) and *tert*-butanol (2-methyl-2-propanol), as well as *sec*-butanol (2-butanol) are the structural (1- and 2-butanol are positional isomers, while isobutanol and *tert*-butanol are chain isomers) isomers of 1-butanol, the primary alcohol with four carbon atoms in molecule. Butanols are important not only as possible co-solvents for CO₂ capture but also as solvents, plasticizers, varnishes, ink component, artificial flavoring, gasoline additive, biofuels, syntheses of other chemical compounds, etc. [9,10].

We continue our study on carbon dioxide + branched alcohols reporting the vapor–liquid critical curves and new isothermal vapor–liquid equilibrium data for carbon dioxide + isobutanol and carbon dioxide + *tert*-butanol, respectively, at 363.15 and 373.15 K and pres-

tures up to 147.3 bar. New data, especially the critical curves, are necessary as the analysis of the available literature data [21,22] showed that there are significant differences among both vapor–liquid equilibrium data and critical curves reported by various research groups. In addition, for both critical curves of carbon dioxide + isobutanol and + *tert*-butanol binary systems are reported few points in a limited range of pressures and temperatures [26–30]. As in our previous studies [21,22] we carefully reviewed the literature for the carbon dioxide + isobutanol and carbon dioxide + *tert*-butanol binary systems, Table 1 summarizes only the data reported afterwards. The available literature critical data are presented in Table 2.

Table 2. Literature experimental critical data for carbon dioxide + isobutanol and + *tert*-butanol.

$P_{\text{range}}/\text{bar}$	$T_{\text{range}}/\text{K}$	N_{exp}	Observations	Reference
carbon dioxide (1) + isobutanol (2)				
147.4 ÷ 122.00	373.15 ÷ 493.15	4	LV	[26]
80.30 ÷ 143.1	313.20 ÷ 353.20	5	LV	[27]
carbon dioxide (1) + <i>tert</i> -butanol (2)				
101.7 ÷ 120.4	323.20 ÷ 353.20	4	LV	[28]
19.5 ÷ 112.9	341.60 ÷ 351.30	2	LV	[29]
92.3 ÷ 111.6	323.20 ÷ 343.20	2	LV	[30]

The new and all available literature data were modeled with the General Equation of State (GEOS) [31,32], Peng–Robinson (PR) [33], and Soave–Redlich–Kwong (SRK) [34] equations of state (EoS) coupled with classical van der Waals mixing rules (two-parameter conventional mixing rule, 2PCMR). The GEOS has four parameters and is a generalization for all cubic EoSs with two, three, and four parameters [31,32]. Instead of correlating the new data, we used one set of binary interaction parameters for each thermodynamic model determined using k_{12} – l_{12} method [35–37] for the carbon dioxide + 2-butanol binary system [37], and we calculated predictively the critical curves and VLE data.

Finally, we analyzed the phase behavior of the carbon dioxide + butanols (+*n*-butanol, +*sec*-butanol, +isobutanol, and +*tert*-butanol) to compare their ability to dissolve carbon dioxide. The experimental and prediction results showed that the molar fraction of carbon dioxide increases in the order 1-butanol < isobutanol < 2-butanol < *tert*-butanol.

2. Materials and Methods

2.1. Materials

Carbon dioxide with purity of min. 0.99995 (mass fraction) was procured from Linde Gaz Romania; isobutanol (purity min. 0.995, in mass fraction) and *tert*-butanol (purity min. 0.995, in mass fraction) were purchased from Sigma-Aldrich, as reported in Table 3. All substances were used without further purification. However, the purity of both alcohols was also tested and confirmed by gas chromatography.

Table 3. Description of materials.

Compound	Chemical Formula	CAS Registry Number	Source	Purification Method	Minimum Mass Fraction Purity
carbon dioxide	CO ₂	124-38-9	Linde Gaz Romania	None	0.99995
isobutanol	C ₄ H ₁₀ O	78-83-1	Sigma-Aldrich	None	>0.995
<i>tert</i> -butanol	C ₄ H ₁₀ O	75-65-0	Sigma-Aldrich	None	>0.995

2.2. Methods

The apparatus and experimental measurement procedures were described in detail in previous papers [38,39]; therefore, only short descriptions are provided.

Apparatus. The static-analytical process with phases (liquid and vapor) sampling was used for the VLE measurements. The main unit of the phase equilibrium apparatus is the high-pressure two opposite sapphire windows cell with adjustable volume, connected with a sampling and analyzing system [38,39]. The sampling system contains two ROLSITM (rapid on-line sampler injector) valves purchased from MINES ParisTech/CEP-TEP—Centre énergétique et procédés, Fontainebleau, France [40]. These two high-pressure electromechanical sampling valves are connected to the equilibrium optical cell and to a gas chromatograph (GC) through thermally insulated capillaries. A heating resistance is used to vaporize rapidly the liquid samples from the expansion chamber of the sampler injector. The transferring lines between ROLSI and the GC are heated with a linear resistor coupled to an Armines/CEP/TEP regulator. The Perichrom gas chromatograph is fitted out with a thermal conductivity detector (TCD) and a 30 m long and 0.530 mm diameter HP-Plot/Q column. The GC carrier gas is Helium at a flow rate between 8 to 30 mL/min. The rig is completed with a syringe pump model 500D from Teledyne ISCO.

Experimental procedure. The isothermal pressure-composition data working procedure was presented in detail previously [6,7]. The procedure starts by rinsing several times with carbon dioxide the equilibrium cell as well the entire internal loop of the apparatus. The next step is to evacuate the gas from the equilibrium cell and the lines with a vacuum pump. After degassing the visual cell by using a vacuum pump and vigorously stirring, the organic compound is charged. The cell is subsequently filled with carbon dioxide using the syringe pump and the pressure is set to the chosen value. Next, the cell is heated to the desired experimental temperature. For a few hours, the mixture in the cell is stirred vigorously to enable the approach to an equilibrium state. The stirrer is then switched off for about 1 h, to ensure the complete separation of the coexisting phases. At this point, samples from both liquid and vapor phases are withdrawn by ROLSI and send to the GC to be analyzed. The repeatability is checked at the equilibrium temperature and pressure by analyzing at least six samples of the liquid phase. As the sample sizes are very small, the equilibrium state is not perturbed and the pressure in the visual cell remains constant.

The calibration of the TCD for CO₂ and butanols is done by injecting known amounts of each component using gas chromatographic syringes (250 µL for the gas, 5 and 10 µL for the liquids). Calibration data are fitted to polynomials to obtain the mole number of the component versus chromatographic area. The correlation coefficients of the GC calibration curves were 0.999 for carbon dioxide and 0.997 for both isobutanol and *tert*-butanol.

The uncertainties in all variables and properties were estimated as described in our previous papers [6,7]. The standard uncertainties are 0.001 and 0.005 for the liquid phase and vapor phase, respectively. The platinum temperature probe (PT-100) is connected to a digital display. It was calibrated against the calibration system Digital Precision Thermometer with PT-100 sensor at the Romanian Bureau of Legal Metrology. The uncertainty of platinum probe is estimated to be within ±0.1 K using a similar method to that explained in references [6,7]. The pressure transducer is connected to a digital multimeter. It was calibrated at 323.15 K with a precision hydraulic dead-weight tester, namely, model 580C, DH-Budenberg SA, Aubervilliers, France. The uncertainty of the pressures is estimated to be within ±0.015 MPa using the method presented previously [6,7], for pressures between (0.5 and 20) MPa.

The critical points were measured in this work using the subsequent procedure. The determination of critical points starts by analyzing the composition at constant temperature and at a sufficiently high pressure, so the system presents a homogeneous phase. Then, the pressure is very slowly modified by adjusting the volume of the cell with the manual pump in order to observe the transition from the homogeneous phase (single phase) to heterogeneous (two phases) and if a bubble or a dew point appears firstly by keeping the temperature constant. If a bubble point is obtained, the temperature is slowly increased until the first dew point is observed, then the pressure is raised to a homogeneous phase, and the composition is determined by sampling. Then, the pressure is very slowly reduced until the first drops of liquid are seen. At this point, the temperature is slowly reduced

simultaneously with decreasing the volume, so the system is at the limit between homogeneous (single phase) and heterogeneous (two phases). The reducing of temperature continues until the first gas bubbles are detected. In this way, the range in which the critical points are located is reduced to 0.2 K and 0.1 bar, compared to the critical opalescence that can be observed in wider ranges of temperature (~5 K) and pressure (~10–15 bar, depending on the system analyzed). The entire procedure is then repeated by adding new quantities of CO₂ and very slowly cooling.

3. Modeling

The phase behavior of carbon dioxide + isobutanol and carbon dioxide + *tert*-butanol was modelled with the General Equation of State (GEOS), Soave–Redlich–Kwong (SRK), and Peng–Robinson (PR) equations of state (EoSs), coupled with classical van der Waals mixing rules (2PCMR).

The GEOS [31,32] equation of state is

$$P = \frac{RT}{V - b} - \frac{a(T)}{(V - d)^2 + c} \tag{1}$$

with the classical van der Waals mixing rules

$$a = \sum_i \sum_j X_i X_j a_{ij} \quad b = \sum_i X_i b_i \tag{2}$$

$$c = \sum_i \sum_j X_i X_j c_{ij} \quad d = \sum_i X_i d_i \tag{3}$$

$$a_{ij} = (a_i a_j)^{\frac{1}{2}} (1 - k_{ij}) \quad b_{ij} = \frac{b_i + b_j}{2} (1 - l_{ij}) \quad c_{ij} = \pm (c_i c_j)^{\frac{1}{2}} \tag{4}$$

with “+” for $c_i, c_j > 0$ and “−” for $c_i, c_j < 0$. Generally, negative values are common for the c parameter of pure components.

The four parameters $a, b, c,$ and d for a pure component are expressed by

$$a(T) = \frac{R^2 T_c^2}{P_c} \beta(T_r) \Omega_a \quad b = \frac{RT_c}{P_c} \Omega_b \tag{5}$$

$$c = \frac{R^2 T_c^2}{P_c^2} \Omega_c \quad d = \frac{RT_c}{P_c} \Omega_d \tag{6}$$

Setting four critical conditions, with α_c as the Riedel criterion:

$$P_r = 1 \quad \left(\frac{\partial P_r}{\partial V_r} \right)_{T_r} = 0 \quad \left(\frac{\partial^2 P_r}{\partial V_r^2} \right)_{T_r} = 0 \quad \alpha_c = \left(\frac{\partial P_r}{\partial T_r} \right)_{V_r} \tag{7}$$

at $T_r = 1$ and $V_r = 1$, the expressions of the parameters $\Omega_a, \Omega_b, \Omega_c, \Omega_d$ are obtained

$$\Omega_a = (1 - B)^3 \quad \Omega_b = Z_c - B \quad \Omega_c = (1 - B)^2 (B - 0.25) \tag{8}$$

$$\Omega_d = Z_c - \frac{(1 - B)}{2} \quad B = \frac{1 + m}{\alpha_c + m} \tag{9}$$

where $P_r, T_r,$ and V_r are the reduced variables, and Z_c is the critical compressibility factor.

The temperature function used is

$$\beta(T_r) = T_r^{-m} \tag{10}$$

GEOS parameters, m and α_c , were calculated by constraining the EoS to reproduce the experimental vapour pressure and liquid volume on the saturation curve between the triple point and the critical point [6,7].

The SRK [34] EoS is

$$P = \frac{RT}{V-b} - \frac{a(T)}{V \cdot (V+b)} \quad (11)$$

where the two parameters, a and b , are

$$a = 0.42748 \frac{R^2 T_c^2}{P_c} \alpha(T) \quad (12)$$

$$b = 0.08664 \frac{RT_c}{P_c} \quad (13)$$

$$\alpha(T_R, \omega) = \left[1 + m_{SRK} (1 - T_R^{0.5}) \right]^2 \quad (14)$$

$$m_{SRK} = 0.480 - 1.574\omega - 0.176\omega^2 \quad (15)$$

The Peng–Robinson [33] equation of state is

$$P = \frac{RT}{V-b} - \frac{a(T)}{V(V+b) + b(V-b)} \quad (16)$$

where the two constants, a and b , are

$$a = 0.45724 \frac{R^2 T_c^2}{P_c} \alpha(T) \quad (17)$$

$$b = 0.077796 \frac{RT_c}{P_c} \quad (18)$$

$$\alpha(T_R, \omega) = \left[1 + m_{PR} (1 - T_R^{0.5}) \right]^2 \quad (19)$$

$$m_{PR} = 0.37464 - 1.54226\omega - 0.26992\omega^2 \quad (20)$$

As Equations (8) and (9) are general forms for all the cubic equations of state with two, three, and four parameters, to obtain the parameters of the SRK EoS, we set the following restrictions: $\Omega_c = -\left(\frac{\Omega_b}{2}\right)^2$ and $\Omega_d = -\frac{\Omega_b}{2}$. From this, it follows:

$$\Omega_c = (1-B)^2(B-0.25) = -\frac{(Z_c-B)^2}{4} \quad (21)$$

$$\Omega_d = Z_c - 0.5(1-B) = -\frac{(Z_c-B)}{2} \quad (22)$$

It results in $Z_c(SRK) = \frac{1}{3}$, and the relation for B (SRK) is

$$B = 0.25 - \frac{1}{36} \left(\frac{1-3B}{1-B} \right)^2 \quad (23)$$

This equation is solved iteratively, and it results $B(SRK) = 0.246$. Correspondingly, for the other parameters we obtained $\Omega_a(SRK) = (1-B)^3 = 0.42748$ and $\Omega_b(SRK) = Z_c - B = 0.08664$.

Similarly, for PR EoS we set the restrictions: $\Omega_c = -2(\Omega_b)^2$ and $\Omega_d = -\Omega_b$. It results in

$$B = 0.25 - \frac{1}{8} \left(\frac{1-3B}{1-B} \right)^2 \quad (24)$$

$$Z_c = \frac{1+B}{4} \quad (25)$$

giving $B(PR) = 0.2296$ and $Z_c(PR) = 0.3074$.

The calculations were made using the software package *PHEQ*, developed in our laboratory [41] and GPEC (Global Phase Equilibrium Calculations) [42–44]. The method proposed by Heidemann and Khalil [45] with numerical derivatives proposed by Stockfleth and Dohrn [46] is implemented in our software to calculate the critical curves.

4. Results and Discussion

4.1. Experimental Results

Vapor–liquid equilibrium compositions for the carbon dioxide + isobutanol and carbon dioxide + *tert*-butanol binary systems were measured at 363.15 and 373.15 K and pressures up to 147.30 and 121.8 bar, respectively. Table 4 presents the new isothermal experimental data together with the corresponding estimated uncertainties for all quantities. To the best of our knowledge, the two isotherms for the carbon dioxide + *tert*-butanol system are for the first time measured, while for carbon dioxide + isobutanol system only the 363.15 K is not reported. The available literature data [26] at 373.15 K for the carbon dioxide + isobutanol binary system are plotted together with our data in Figure 1. Some differences can be observed between our data and those measured by reference [26] for the liquid phase. It should be mentioned that the reported uncertainty of their phase compositions is $\pm 1.0\%$ [20]. However, the new data are in good agreement with our previous measurements [21,22].

Table 4. Mole fraction of component 1 in the liquid phase, X_1 , and mole fraction of component 1 in the vapor phase, Y_1 , at various temperatures, T , and pressures, P , for the binary system carbon dioxide (1) + isobutanol (2) and carbon dioxide (1) + *tert*-butanol (2).

P/bar	X_1	Y_1	P/bar	X_1	Y_1
carbon dioxide (1) + isobutanol (2)			carbon dioxide (1) + <i>tert</i> -butanol (2)		
$T/\text{K} = 363.15 \pm 0.1$					
20.90	0.1139	0.9770	19.30	0.1129	0.9612
31.00	0.1454	0.9901	31.10	0.1926	0.9706
45.60	0.2115	0.9872	45.10	0.2822	0.9779
60.90	0.2838	0.9953	60.60	0.3790	0.9879
76.70	0.3683	0.9887	76.10	0.4919	0.9846
90.90	0.4439	0.9834	90.40	0.5819	0.9638
106.35	0.5232	0.9726	105.80	0.6834	0.9389
120.30	0.5947	0.9578	119.00	0.8303	0.8812
131.50	0.6867	0.9377	118.90 ^a	0.8980	0.8980
142.10 ^a	0.8781	0.8781			
$T/\text{K} = 373.15 \pm 0.1$					
33.50	0.1634	0.9724	15.30	0.0838	0.8922
56.10	0.2521	0.9782	30.40	0.1786	0.9591
79.90	0.3590	0.9819	45.60	0.2703	0.9434
95.50	0.4320	0.9800	60.20	0.3586	0.9729
110.10	0.5054	0.9646	75.60	0.4566	0.9817
125.10	0.5832	0.9508	91.30	0.5510	0.9602
140.50	0.7062	0.9194	105.50	0.6287	0.9466
147.30 ^a	0.8564	0.8564	118.60	0.7344	0.9067
			121.80 ^a	0.8798	0.8798

Standard uncertainties: $u(T) = 0.1$ K, $u(P) = 0.1$ bar, $u(X_1) = 0.001$, $u(Y_1) = 0.005$. ^a Critical points.

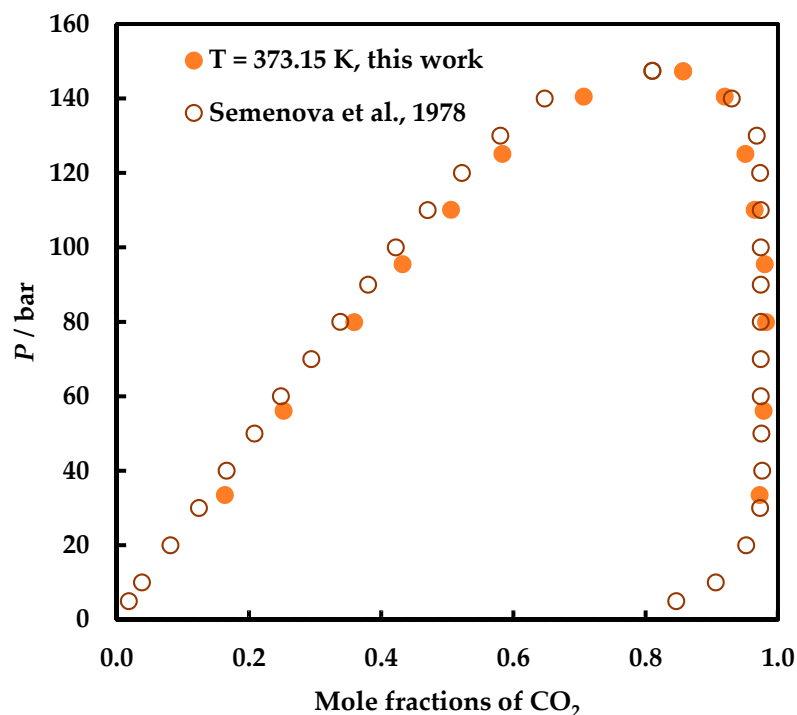


Figure 1. Comparison of measured and literature data [26] for carbon dioxide (1) + isobutanol (2) system at 373.15 K.

In Figure 2, we compare experimental data of carbon dioxide + 1-butanol binary system [47], as well as for all $C_4H_{10}O$ isomers, i.e., carbon dioxide + 2-butanol [47], carbon dioxide + isobutanol, and carbon dioxide + *tert*-butanol systems at the same temperature, 363.15 K.

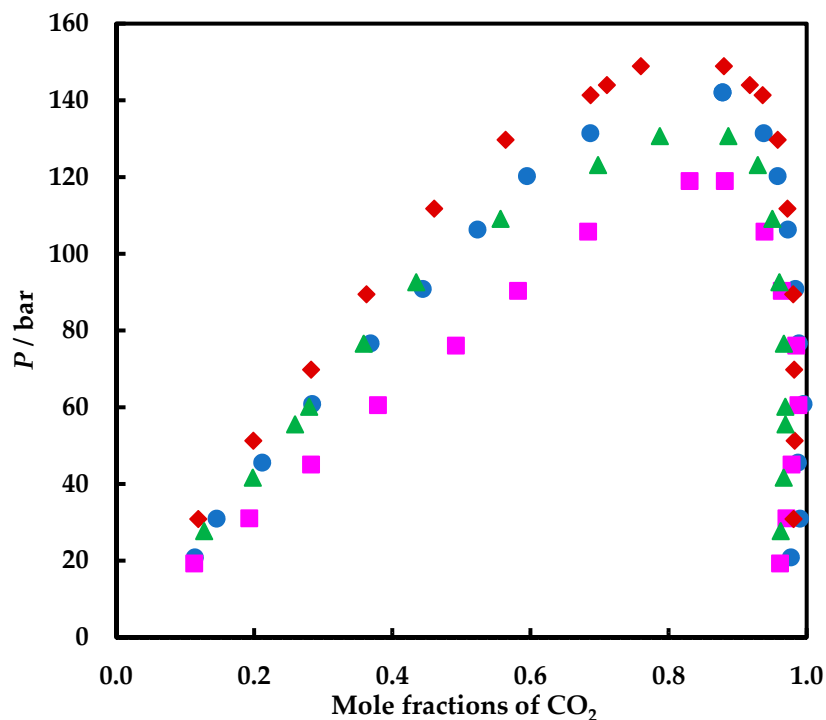


Figure 2. Comparison of measured and literature data for carbon dioxide (1) + 1-butanol (2), + 2-butanol (2), + isobutanol (2), and + *tert*-butanol (2) binary systems at 363.15 K. CO_2 + 1-butanol: \blacklozenge , [47]; CO_2 + 2-butanol: \blacktriangle [47]; CO_2 + isobutanol: \bullet this work; CO_2 + *tert*-butanol: \blacksquare , this work.

It can be observed that our experimental data for carbon dioxide + isobutanol and + *tert*-butanol are in good agreement with those reported by Galicia-Luna et al. [47] for carbon dioxide + 1-butanol and + 2-butanol, respectively. At higher pressures, the solubility of carbon dioxide increases in the order 1-butanol < isobutanol < 2-butanol < *tert*-butanol, as observed by other researchers [23]. Although the differences in compositions are small, especially between 2-butanol and isobutanol, this correlation opens new perspectives for applications, such as isomers separation based on pressure difference [23].

Furthermore, the new isothermal data for both systems are also shown in Figure 3. Thus, Figure 3a compares the data measured at 363.15 K for both carbon dioxide + isobutanol and carbon dioxide + *tert*-butanol, while Figure 3b shows data determined at 373.15 K. At both temperatures, carbon dioxide is more soluble in *tert*-butanol in the liquid phase, and its solubility increases with an increase in the pressure.

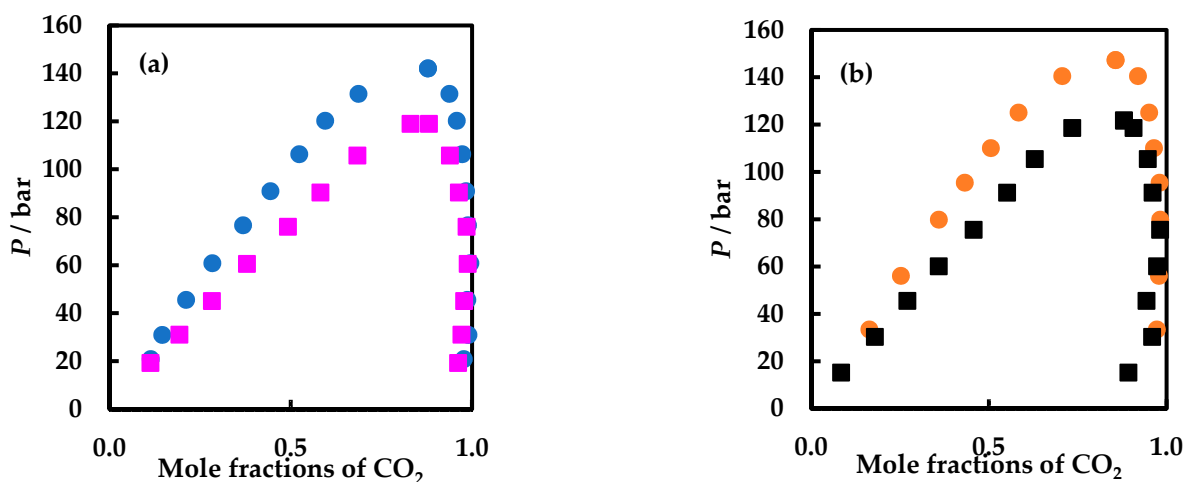


Figure 3. Pressure–compositions data for the carbon dioxide + isobutanol and + *tert*-butanol systems at 363.15 K (a) and 373.15 K (b): (●, ○), CO₂ + isobutanol; (■, ■), CO₂ + *tert*-butanol.

We also measured the vapor–liquid critical curves starting from the critical point of carbon dioxide up to 373.15 and 147.3 bar for carbon dioxide + isobutanol binary system and up to 405.15 K and 121.4 bar for carbon dioxide + *tert*-butanol binary system, values which are near or over the critical pressure maximum (CPM). The new critical data are presented in Table 5 and plotted in Figure 4. In the same figure we drew the critical temperatures and pressures for both systems available from literature. Thus, Semenova et al. [26] reported four critical points at high temperatures and Wang et al. [27] estimated five critical points at temperatures closer to the critical point of carbon dioxide for the carbon dioxide + isobutanol system. Wang et al. [28] estimated four points, while Chen et al. [29] and Kim et al. [30] estimated only two points each for the carbon dioxide + *tert*-butanol system.

In Figure 5, we compare the LV critical curves for carbon dioxide + all butanol isomers. The miscibility gap increases in the order *tert*-butanol < 2-butanol < isobutanol < 1-butanol. The critical data reported for the carbon dioxide + isobutanol and carbon dioxide + *tert*-butanol binary systems agree very well with the data measured for carbon dioxide + 1-butanol and carbon dioxide + 2-butanol binary systems. Experimental data, including critical compositions, are reported for the entire temperature range for the carbon dioxide + 2-butanol system [48,49], while for the carbon dioxide + 1-butanol binary system critical pressures and temperatures are available almost in the entire temperature range from Ziegler et al. [50] and Yeo et al. [51]. Gurdial et al. [52] measured several critical data for the carbon dioxide + 1-butanol system at temperatures closer to the critical point of carbon dioxide.

4.2. Modelling Results

The new and literature data for carbon dioxide + isobutanol and carbon dioxide + *tert*-butanol were predictively modeled with three thermodynamic models, namely, GEOS, PR, and SRK EoSs coupled with classical van der Waals mixing rules.

Recently, we showed that the binary interaction parameters (k_{12} and l_{12}) determined by the k_{12} - l_{12} method [35–37] for the carbon dioxide + 2-butanol binary system can be successfully used to model either carbon dioxide + different organic substances containing four C atoms without and with one or two oxygen atoms (*n*-butane, 1-butanol, 1,2-dimethoxyethane, ethyl acetate, dioxane [5–8]), either carbon dioxide + a lower member of the same homologous series, i.e., 2-propanol [53].

The carbon dioxide + 2-butanol binary system can be used as a model system as critical data are available in the entire range, including the UCEP and LLV [48].

Here, we use the same modeling procedure, and we calculated the critical curves and VLE data for the two systems containing carbon dioxide and the chain isomers, isobutanol and *tert*-butanol, using the binary interaction parameters determined for the carbon dioxide + 2-butanol binary system [37] for each thermodynamic model. These parameters are presented in Table 6.

It should be noted that the parameters from Table 6 were determined using the values of pure components (CO₂, 2-butanol) critical data and acentric factors from Reid et al. [54]. Therefore, we recalculated the critical curve using the binary interaction parameters (BIPs) from Table 6 for the carbon dioxide + 2-butanol system using the pure components critical data and acentric factors from both Poling et al. [55] and DIPPR [56] database.

Table 5. Critical points data carbon dioxide (1) + isobutanol (2) and carbon dioxide (1) + *tert*-butanol (2) binary systems ^a.

<i>T</i> /K	<i>P</i> /bar	<i>X</i> ₁	<i>T</i> /K	<i>P</i> /bar	<i>X</i> ₁
carbon dioxide + isobutanol			carbon dioxide + <i>tert</i> -butanol		
304.21 ^b	73.83	1.0000	304.21 ^b	73.83	1.0000
316.65	87.20		320.45	87.40	0.9715
317.05	87.50		323.15 ^c	89.90	0.9687
318.15	89.00		326.25	92.90	0.9630
320.15	91.60		330.75	96.80	0.9570
327.60	101.60		333.15 ^c	99.20	0.9528
332.95	109.60		337.85	102.30	0.9477
335.25	112.30		341.85	105.40	0.9420
339.25	117.30		343.15 ^c	106.80	0.9408
348.50	128.65		346.75	109.20	0.9332
353.35	133.80		352.35	112.50	0.9218
353.50	134.05		353.15 ^c	112.90	0.9215
356.85	137.00		362.65	118.20	0.8994
359.05	138.40		363.15	118.90	0.8980
363.15	142.10	0.8781	373.15	121.80	0.8798
364.15	142.40		375.95	122.90	0.8738
367.65	144.70		381.35	124.00	0.8563
369.35	145.70		387.65	124.60	0.8371
371.65	146.90		395.55	124.70	0.8047
373.15	147.30	0.8564	399.75	124.50	0.7821
547.80 ^b	42.95	0.0000	405.15	121.40	0.7417
			506.20 ^b	39.72	0.0000

^a $u(T) = 0.1$ K, $u(P) = 0.1$ bar, $u(X_1) = 0.001$. ^b DIPPR [56] values. ^c Measured in our group [21,22].

Table 6. Binary interaction parameters used in calculations [37].

EoS	k_{12}	l_{12}
GEOS	0.050	−0.040
PR	0.025	−0.108
SRK	0.020	−0.111

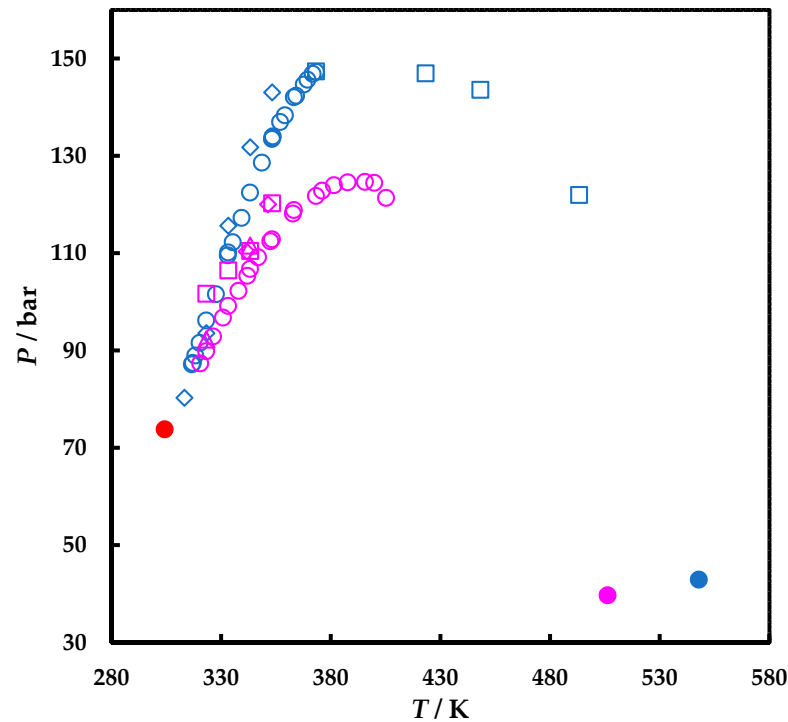


Figure 4. P – T fluid phase diagram of the carbon dioxide (1) + isobutanol (2) and carbon dioxide (1) + *tert*-butanol (2) systems. Critical points (CP) of pure components: ●, CP CO₂ [56]; ●, CP isobutanol [56]; ●, CP *tert*-butanol [56]. CP CO₂ + isobutanol: ○, this work; □, [26]; ◇, [27]. CP CO₂ + *tert*-butanol: ○, this work; □, [28]; ◇, [29]; △, [30].

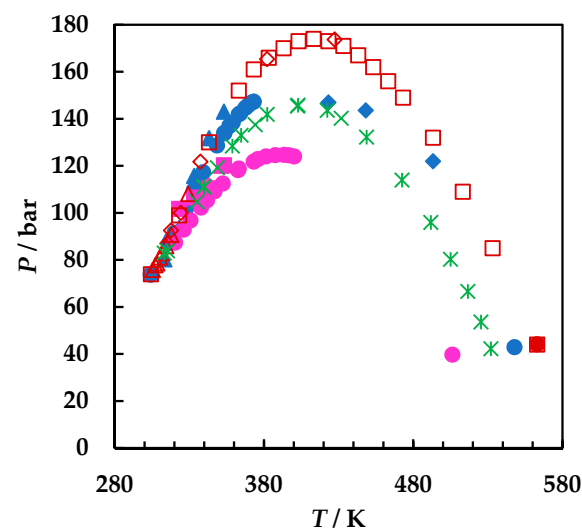


Figure 5. P – T fluid phase diagram of the carbon dioxide (1) + *tert*-butanol (2), carbon dioxide (1) + 2-butanol (2), carbon dioxide (1) + isobutanol (2), and carbon dioxide (1) + 1-butanol (2) binary systems. The symbols represent the binary systems as follows: CO₂ + *tert*-butanol (●, this work; ■, [28]; ▲, [29]; ◆, [30]); CO₂ + 2-butanol (*, [48]; ×, [49]); CO₂ + isobutanol (●, this work; ▲, [27]; ◆, [26]); CO₂ + 1-butanol (△, [52]; □, [50]; ◇, [51]).

In Table 7, we compiled the critical data and acentric factors for all butanol isomers and carbon dioxide from the three sources mentioned, while in Tables 8 and 9 we provided all GEOS parameters (m , α_c , Ω_a , Ω_b , Ω_c , and Ω_d).

Table 7. Critical parameters (T_c , P_c , V_c) and acentric factor (ω) for pure components.

Database	Reid et al. [54]				Poling et al. [55]				DIPPR [56]			
Substance	T_c /K	P_c /bar	V_c /cm ³ /mol	ω	T_c /K	P_c /bar	V_c /cm ³ /mol	ω	T_c /K	P_c /bar	V_c /cm ³ /mol	ω
carbon dioxide	304.10	73.80	93.9	0.239	304.12	73.74	94.07	0.225	304.21	73.83	94	0.223621
1-butanol	563.10	44.20	275	0.593	563.05	44.23	275	0.590	563.1	44.14	273	0.588280
2-butanol	536.10	41.80	269	0.577	536.05	41.79	269	0.574	535.9	42.02	270	0.580832
isobutanol	547.80	43.00	273	0.592	547.78	43.00	273	0.590	547.8	42.95	274	0.585710
tert-butanol	506.20	39.70	275	0.612	506.21	39.73	275	0.613	506.2	39.72	275	0.615203

Table 8. GEOS parameters (α_c , m) for pure components.

Substance	m	α_c
carbon dioxide	0.3146	7.0517
1-butanol	0.6437	9.0580
2-butanol	0.6533	9.0298
isobutanol	0.6005	9.9243
tert-butanol	0.6814	9.1161

Table 9. The critical compressibility factor (Z_c), and GEOS parameters (Ω_a , Ω_b , Ω_c , Ω_d , B).

EoS	GEOS					PR	SRK
Substance	CO ₂	1-butanol	2-butanol	isobutanol	tert-butanol	all	all
B	0.1785	1.3342	1.3396	0.1521	0.1716	0.2467	0.2296
Z_c	0.2746	0.2576	0.2540	0.2586	0.2597	0.3333	0.3074
Ω_a	0.5545	−0.0373	−0.0392	0.6097	0.5685	0.4275	0.4572
Ω_b	0.0961	−1.0766	−1.0857	0.1065	0.0881	0.0866	0.0778
Ω_c	−0.0483	0.1211	0.1257	−0.0704	−0.0538	−0.0187	−0.0121
Ω_d	−0.1362	0.4247	0.4238	−0.1654	−0.1545	−0.0434	−0.0778

The differences in critical maximum pressures are very small for all three EoSs, and hence, we decided to use the BIPs from Table 6 in combination with the critical data and acentric factors from DIPPR [56], presented in Table 7, as recommended by other researchers [57].

Moreover, in a recent paper [6], we studied the effect of critical parameters and acentric factors of pure components from different database for carbon dioxide + dioxane (C₄H₈O₂) binary mixture, and we showed that the differences are small for the VLE calculations.

In Figure 6, we compare the model results with the critical experimental data for all butanol binary systems. PR and SRK EoSs behave similarly for all systems, and the CPMs are slightly shifted to the right compared with the experimental ones, while the GEOS reproduces better the CPMs, except for carbon dioxide + isobutanol system. As the figure is busy, we compare the new data with the chosen reference model, carbon dioxide + 2-butanol system, and the predictions by the GEOS and PR in Figure 7. The predictions for the carbon dioxide + tert-butanol binary system are very good for all three models (Figure 7b), while for the carbon dioxide + isobutanol system (Figure 7a) GEOS seems to overpredict the CPM, but the corresponding temperature is closer to the experimental one. Both PR and SRK also overpredict the CPM, but at a lower pressure and at higher temperature than the GEOS for the carbon dioxide + isobutanol binary system.

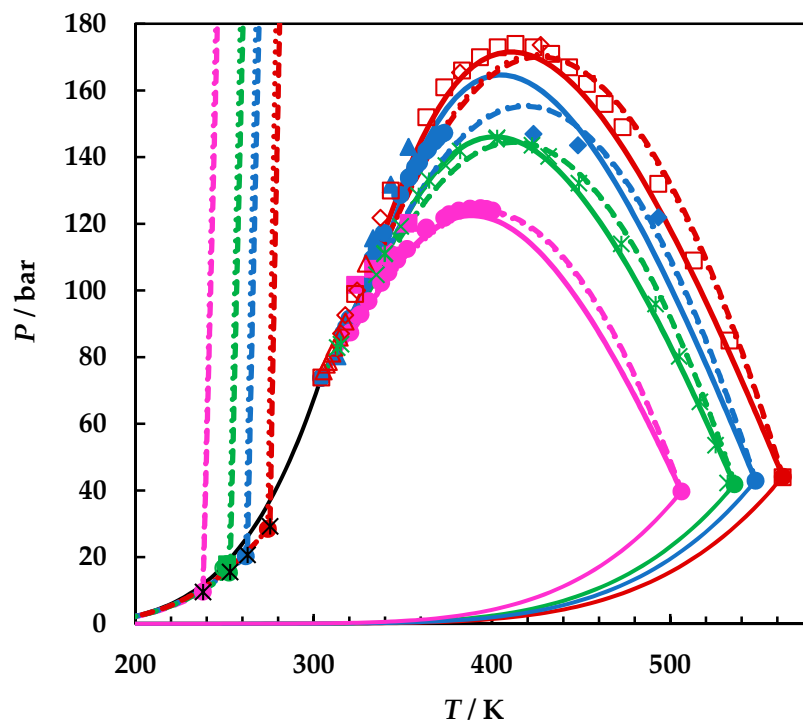


Figure 6. P – T fluid phase diagram of the carbon dioxide (1) + *tert*-butanol (2), +2-butanol (2), + isobutanol (2), and +1-butanol (2) binary systems. Experimental data: CO₂ + *tert*-butanol (●, this work; ■, [28]; ▲, [29]; ◆, [30]); +2-butanol (*, [48]; ×, [49]); + isobutanol (●, this work; ▲, [27]; ◆, [26]); +1-butanol (▲, [52]; □, [50]; ◇, [51]). Model results: GEOS (full lines); PR (dotted lines); SRK (dashed lines).

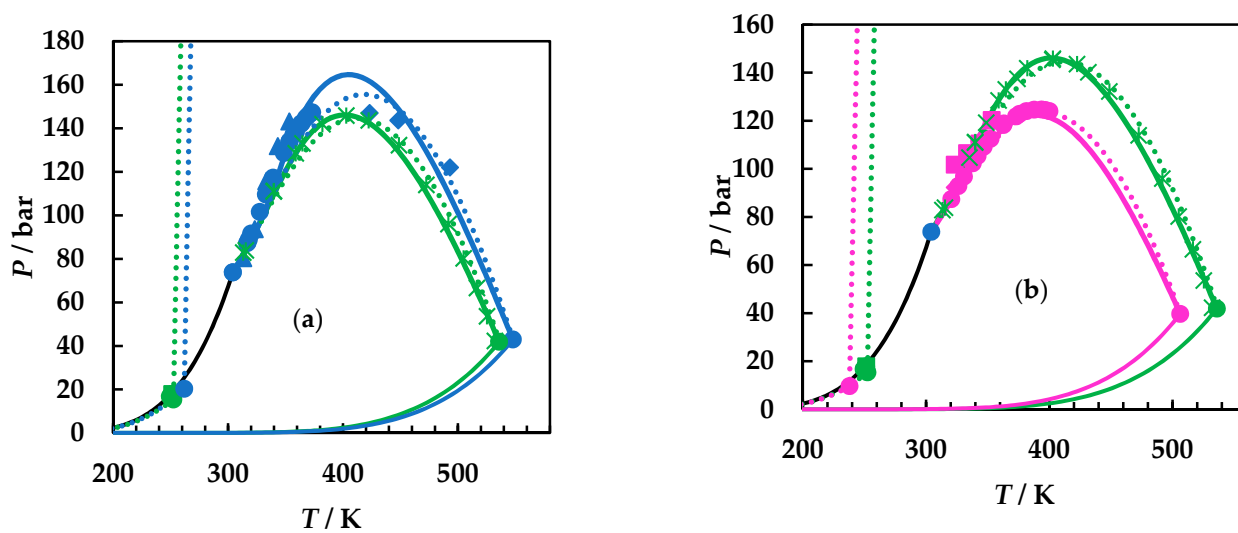


Figure 7. Cont.

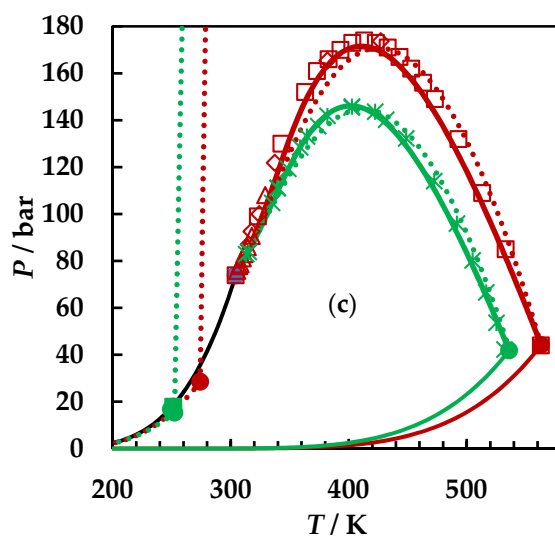


Figure 7. P – T fluid phase diagram of the carbon dioxide (1) + *tert*-butanol (2) and carbon dioxide (1) + 2-butanol (2) (a), carbon dioxide (1) + isobutanol (2) and carbon dioxide (1) + 2-butanol (2) (b), and carbon dioxide (1) + 1-butanol (2) and carbon dioxide + 2-butanol (2) binary systems (c). Experimental data: CO₂ + *tert*-butanol (●, this work; ■, [28]; ▲, [29]; ◆, [30]); CO₂ + 2-butanol (*, [48]; ×, [49]); CO₂ + isobutanol (●, this work; ▲, [27]; ◆, [26]); CO₂ + 1-butanol (△, [52]; □, [50]; ◇, [51]). Model results: GEOS (full lines); PR (dotted lines).

The LV critical curve of the carbon dioxide + 1-butanol system is very well reproduced by all three thermodynamic models (Figure 7c), only the temperature corresponding to the CPM is slightly higher than the experimental one for PR and SRK equations of state.

It must be noted that both PR and SRK predict type II phase behavior for all four systems. However, clear experimental evidence exists only for the carbon dioxide + 2-butanol system [48], while for the carbon dioxide + 1-butanol and carbon dioxide + isobutanol Büchner [58] reported in 1906 few liquid–liquid equilibrium points (temperature and the composition of liquid 1) at very low temperature (251.15 K for carbon dioxide + isobutanol and 253.15 to 256.15 K for carbon dioxide + 1-butanol system) [20]. On the other hand, *tert*-butanol has a very high freezing point of about 25.5 °C which can mask any observation of an LLV equilibrium for its binary mixture with carbon dioxide. Therefore, it can be assumed that all carbon dioxide + butanol systems belong to type II phase behavior. However, without knowing the UCEP's temperature, the k_{12} – l_{12} method cannot be applied directly to the carbon dioxide + isobutanol and carbon dioxide + *tert*-butanol binary systems.

The BIPs from Table 6 were also used to predict the new and available VLE data for the carbon dioxide + isobutanol and carbon dioxide + *tert*-butanol binary systems with the GEOS, PR, and SRK models. Considering that the predictions were made with the binary interaction parameters tailored for the carbon dioxide + 2-butanol system and from the P – T global diagrams, it is expected that they will be primarily qualitative for the structural isomers, carbon dioxide + isobutanol and carbon dioxide + *tert*-butanol binary systems. Still, the predictions by GEOS, PR, and SRK EoSs are remarkably good, especially for the carbon dioxide + *tert*-butanol system. As an example, we illustrated the prediction results at 363.15 and 373.15 K for carbon dioxide + isobutanol (Figure 8a) and carbon dioxide + *tert*-butanol (Figure 8b), comparing the new data and all three thermodynamic models used, in Figure 8.

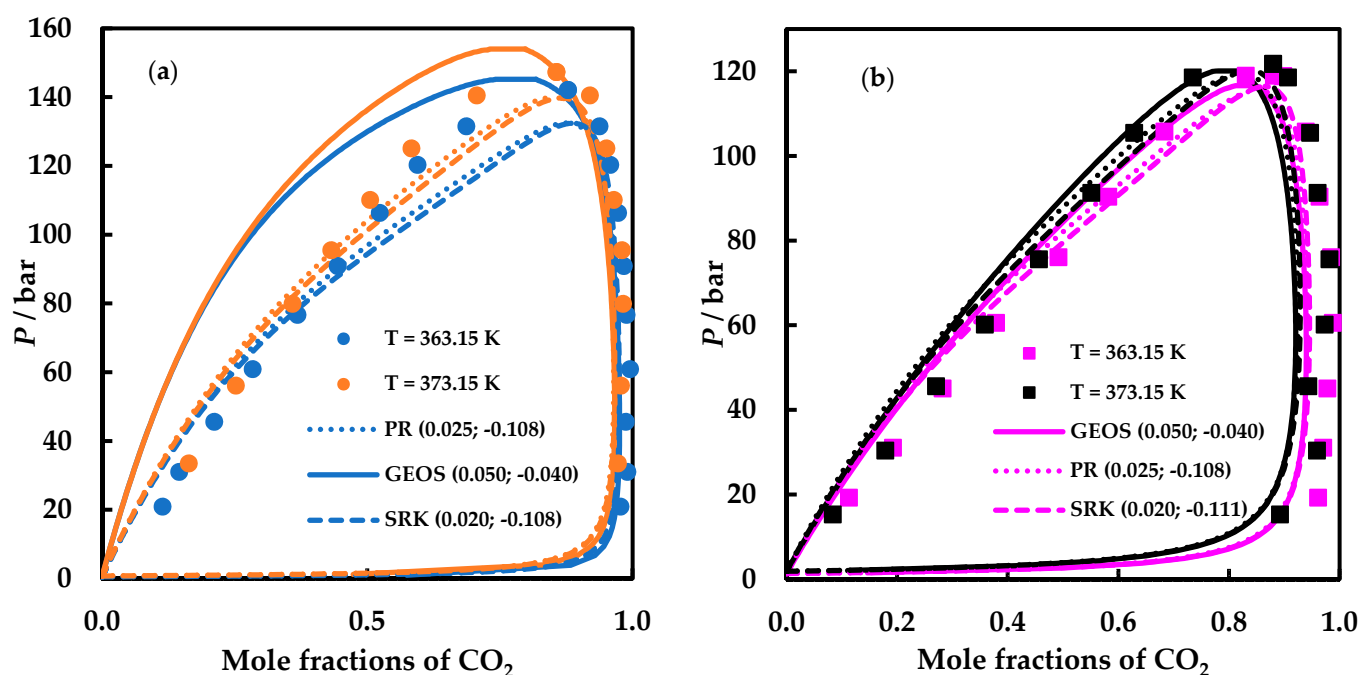


Figure 8. Comparison of new data and predictions by GEOS (full lines), PR (dotted lines), and SRK (dashed lines): (a) carbon dioxide (1) + isobutanol (2) and (b) carbon dioxide (1) + *tert*-butanol (2).

The three models present similar trends for both systems, except for the GEOS equation which shows a lower solubility than the experimental one in the liquid phase for the carbon dioxide + isobutanol system. This behavior is consistent with the inflection observed on the first part of the liquid–vapor critical curve, starting from the critical point of carbon dioxide towards the CPM. It should be also noted that the composition of the vapor phase is underestimated by all models, but it is significantly smaller compared with the experimental values for the carbon dioxide + *tert*-butanol system.

The prediction results are satisfactory for the carbon dioxide + 1-butanol binary system. In Figure 9, we exemplified at 363.15 the calculations by PR EoS for carbon dioxide + 1-butanol, carbon dioxide + 2-butanol, carbon dioxide + isobutanol, and carbon dioxide + *tert*-butanol binary systems. Although the composition of the liquid phase is systematically underpredicted at higher pressures for all systems, the solubility increases in the same order 1-butanol < isobutanol < 2-butanol < *tert*-butanol. The prediction results are encouraging and open the path to obtain at least qualitative information when experimental data are not available.

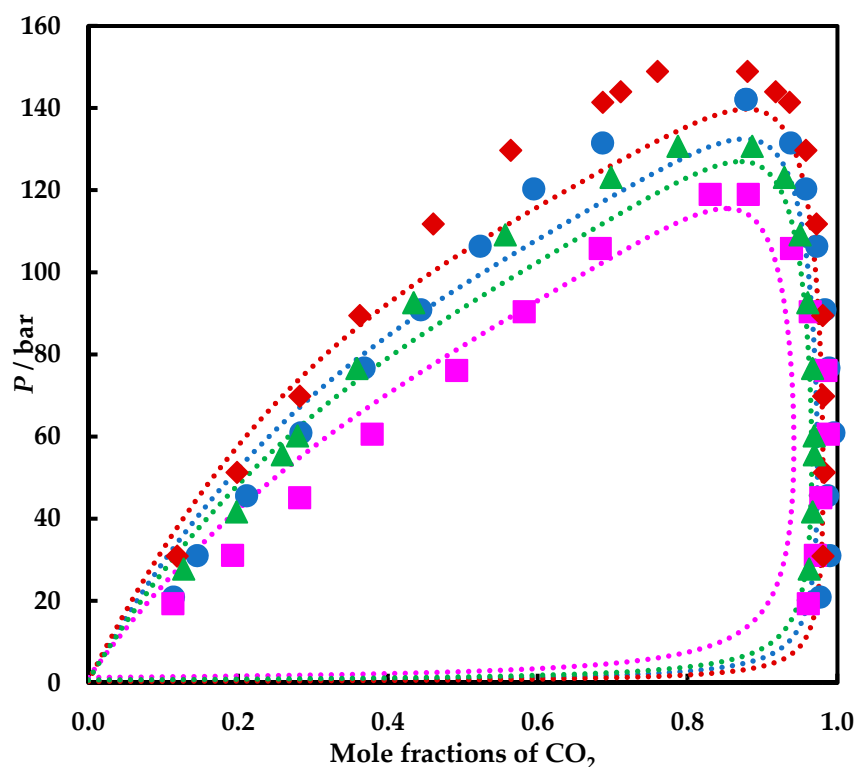


Figure 9. Comparison of experimental data (symbols) for carbon dioxide + 1-butanol, + 2-butanol, + isobutanol, and + *tert*-butanol and predictions (dotted lines) by PR EoS ($k_{12} = 0.025$; $l_{12} = -0.108$).

5. Conclusions

New isothermal vapor–liquid equilibrium data for the carbon dioxide + isobutanol and carbon dioxide + *tert*-butanol system were measured with a visual high-pressure static-analytic setup at 363.15 and 373.15 K. The vapor–liquid critical curves were also measured at pressures up to 147.3 bar and 373.15 K for the carbon dioxide + isobutanol system and up to 121.4 bar and 405.15 K for the carbon dioxide + *tert*-butanol system. The new data are consistent with our previous measurements for the same systems. The General Equation of State, Soave–Redlich–Kwong, and Peng–Robinson equations of state coupled with classical van der Waals mixing rules were used to model the phase behavior of these systems in a predictive manner. Unique sets of binary interaction parameters obtained by the k_{12} - l_{12} method for the carbon dioxide + 2-butanol system were used to model the carbon dioxide + isobutanol and carbon dioxide + *tert*-butanol systems. 2-Butanol, isobutanol, and *tert*-butanol are the structural isomers for 1-butanol, and their binaries with carbon dioxide could be attributed to type II phase behavior. All models predict reasonably well the phase behavior of carbon dioxide + butanols.

The experimental data and the thermodynamic models suggest that the solubility increases in the order 1-butanol < isobutanol < 2-butanol < *tert*-butanol.

Author Contributions: Conceptualization, C.S. and S.S.; methodology, S.S.; software, A.V.C. and C.S.; validation, S.S., A.V.C. and C.S.; writing, C.S.; supervision, C.S.; funding acquisition, C.S. All authors have read and agreed to the published version of the manuscript.

Funding: This work was supported by a grant of Ministry of Research and Innovation, CNCS-UEFISCDI, project number PN-III-P4-ID-PCE-2016-0629, within PNCDI III.

Institutional Review Board Statement: Not applicable.

Informed Consent Statement: Not applicable.

Data Availability Statement: Not applicable.

Acknowledgments: C. Secuianu thanks M. Trusler for constant support.

Conflicts of Interest: The authors declare no conflict of interest. The funders had no role in the design of the study; in the collection, analyses, or interpretation of data; in the writing of the manuscript; or in the decision to publish the results.

References

1. Abanades, J.C.; Rubin, E.S.; Mazzotti, M.; Herzog, H.J. On the climate change mitigation potential of CO₂ conversion to fuels. *Energy Environ. Sci.* **2017**, *10*, 2491–2499. [[CrossRef](#)]
2. Peper, S.; Fonseca, J.M.S.; Dohrn, R. High-pressure fluid-phase equilibria: Trends, recent developments and systems investigated (2009–2012). *Fluid Phase Equilib.* **2019**, *484*, 126–224. [[CrossRef](#)]
3. Uhlemann, J.; Costa, R.; Charpentier, J.-C. Product design and engineering—past, present, future trends in teaching, research and practices: Academic and industry points of view. *Curr. Opin. Chem. Eng.* **2020**, *27*, 10–21. [[CrossRef](#)]
4. Kontogeorgis, G.M.; Dohrn, R.; Economou, I.G.; de Hemptinne, J.-C.; ten Kate, A.; Kuitunen, S.; Mooijer, M.; Zilnik, L.F.; Vesovic, V. Industrial Requirements for Thermodynamic and Transport Properties: 2020. *Ind. Eng. Chem. Res.* **2021**, *60*, 4987–5013. [[CrossRef](#)] [[PubMed](#)]
5. Sima, S.; Secuianu, C. The Effect of Functional Groups on the Phase Behavior of Carbon Dioxide Binaries and Their Role in CCS. *Molecules* **2021**, *26*, 3733. [[CrossRef](#)] [[PubMed](#)]
6. Sima, S.; Secuianu, C.; Nichita, D.V. High-pressure phase equilibria of carbon dioxide + 1,4-dioxane binary system. *Fluid Phase Equilib.* **2021**, *547*, 113181. [[CrossRef](#)]
7. Sima, S.; Cismondi, M.; Secuianu, C. High-Pressure Phase Equilibrium for Carbon Dioxide + Ethyl n-Butyrate Binary System. *J. Chem. Eng. Data* **2021**, *66*, 4094–4102. [[CrossRef](#)]
8. Ioniță, M.; Crișciu, A.; Racoviță, R.C.; Sima, S.; Secuianu, C. Phase diagram predictions for carbon dioxide + different classes of organic substances at high pressures. *U.P.B. Sci. Bull. Ser. B* **2021**, *83*, 117–132.
9. Latsky, C.; Schwarz, C.E. Measurement and modelling of high pressure bubble- and dew-point data for the CO₂ + 1-decanol + 3,7-dimethyl-1-octanol system. *Fluid Phase Equilib.* **2019**, *488*, 87–98. [[CrossRef](#)]
10. Latsky, C.; Mabena, N.S.; Schwarz, C.E. High pressure phase behaviour for the CO₂ + n-dodecane + 3,7-dimethyl-1-octanol system. *J. Supercrit. Fluids* **2019**, *149*, 138–150. [[CrossRef](#)]
11. van Konynenburg, P.H.; Scott, R.L. Critical lines and phase equilibria in binary van der Waals mixtures. *Philos. Trans. R. Soc. Lond. Ser. A* **1980**, *298*, 495–540. [[CrossRef](#)]
12. Privat, R.; Jaubert, J.N. Classification of global fluid-phase equilibrium behaviors in binary systems. *Chem. Eng. Res. Des.* **2013**, *91*, 1807–1839. [[CrossRef](#)]
13. Schwarz, C.E. High Pressure Phase Behavior of the Homologous Series CO₂ + 1-Alcohols. *J. Chem. Eng. Data* **2018**, *63*, 2451–2466. [[CrossRef](#)]
14. Secuianu, C.; Feroiu, V.; Geana, D. Measurements and Modeling of High-Pressure Phase Behavior of the Carbon Dioxide +Pentan-1-ol Binary System. *J. Chem. Eng. Data* **2011**, *56*, 5000–5007. [[CrossRef](#)]
15. Sima, S.; Ioniță, S.; Secuianu, C.; Feroiu, V.; Geana, D. High pressure phase equilibria of carbon dioxide + 1-octanol binary system. *J. Chem. Eng. Data* **2018**, *63*, 1109–1122. [[CrossRef](#)]
16. Dohrn, R.; Brunner, G. High-pressure fluid phase equilibria: Experimental methods and systems investigated (1988–1993). *Fluid Phase Equilib.* **1995**, *106*, 213–282. [[CrossRef](#)]
17. Christov, M.; Dohrn, R. Review. High-pressure fluid phase equilibria. Experimental methods and systems investigated (1994–1999). *Fluid Phase Equilib.* **2002**, *202*, 153–218. [[CrossRef](#)]
18. Dohrn, R.; Peper, S.; Fonseca, J.M.S. High-pressure fluid-phase equilibria: Experimental methods and systems investigated (2000–2004). *Fluid Phase Equilib.* **2010**, *288*, 1–54. [[CrossRef](#)]
19. Fonseca, J.M.S.; Ralf Dohrn, R.; Peper, S. High-pressure fluid-phase equilibria: Experimental methods and systems investigated (2005–2008). *Fluid Phase Equilib.* **2011**, *300*, 1–69. [[CrossRef](#)]
20. *DETERM Database*; DECHEMA Chemistry Data Series; DECHEMA: Frankfurt, Germany, 1991–2021.
21. Sima, S.; Secuianu, C.; Feroiu, V.; Geană, D. New high-pressures vapor-liquid equilibrium data for the carbon dioxide + 2-methyl-1-propanol (isobutanol) binary system. *Cent. Eur. J. Chem.* **2014**, *12*, 953–961. [[CrossRef](#)]
22. Sima, S.; Secuianu, C.; Feroiu, V.; Geană, D. New high-pressures vapor-liquid equilibrium data for the carbon dioxide + 2-methyl-2-propanol binary system. *Cent. Eur. J. Chem.* **2014**, *12*, 893–900. [[CrossRef](#)]
23. Kodama, D.; Kato, M.; Kaneko, T. Volumetric behavior of carbon dioxide + 2-methyl-1-propanol and carbon dioxide + 2-methyl-2-propanol mixtures at 313.15 K. *Fluid Phase Equilib.* **2013**, *357*, 57–63. [[CrossRef](#)]
24. Ferreira, M.O.; Ferreira-Pinto, L.; Souza, E.M.B.D.; Castier, M.; Voll, F.A.P.; Cabral, V.F.; Cardozo-Filho, L. Experimental Vapor-Liquid Equilibria for the Systems 2-Ethyl-1-hexanol + Glycerol + CO₂ and 2-Methyl-2-propanol + Glycerol + CO₂. *J. Chem. Eng. Data* **2013**, *58*, 2506–2512. [[CrossRef](#)]
25. Aida, T.; Aizawa, T.; Kanakubo, M.; Nanjo, H. Relation between Volume Expansion and Hydrogen Bond Networks for CO₂-Alcohol Mixtures at 40 °C. *J. Phys. Chem. B* **2010**, *114*, 13628–13636. [[CrossRef](#)] [[PubMed](#)]
26. Semenova, A.I.; Emelyanova, E.A.; Tsimmerman, S.S.; Tsiklis, D.S. Phase equilibria in the system isobutyl alcohol-carbon dioxide. *Zhurnal Fizicheskoi Khimii* **1978**, *52*, 1149–1152, (accessed via DETHERM).

27. Wang, L.; Hao, X.; Zheng, L.; Chen, K. Phase Equilibrium of Isobutanol in Supercritical CO₂. *Chin. J. Chem. Eng.* **2009**, *17*, 642–647. [[CrossRef](#)]
28. Wang, L.; Li, R.L.; Sun, L.T.; Chen, K.X. Studies on Phase Equilibrium of Tertbutanol in Supercritical CO₂. *Chem. J. Chin. Univ.* **2009**, *30*, 1631–1635.
29. Chen, H.-I.; Chen, P.-H.; Chang, H.-Y. High-Pressure Vapor-Liquid Equilibria for CO₂ + 2-Butanol, CO₂ + Isobutanol, and CO₂ + tert-Butanol Systems. *J. Chem. Eng. Data* **2003**, *48*, 1407–1412. [[CrossRef](#)]
30. Kim, J.S.; Yoon, J.H.; Lee, H. High-Pressure Phase Equilibria for Carbon Dioxide+Methyl-2-propanol and Carbon Dioxide-2-Methyl-2-propanol-Water: Measurement and Prediction. *Fluid Phase Equilib.* **1994**, *101*, 237–245. [[CrossRef](#)]
31. Geană, D. A new equation of state for fluids. I. Applications to PVT calculations for pure fluids. *Rev. Chim.* **1986**, *37*, 303–309.
32. Geană, D. A new equation of state for fluids. II. Applications to phase equilibria. *Rev. Chim.* **1986**, *37*, 951–959.
33. Peng, D.Y.; Robinson, D.B. A new two-constant Equation of State. *Ind. Eng. Chem. Fundam.* **1976**, *15*, 59–64. [[CrossRef](#)]
34. Soave, G. Equilibrium constants from a modified Redlich-Kwong equation of state. *Chem. Eng. Sci.* **1972**, *27*, 1197–1203. [[CrossRef](#)]
35. Polishuk, I.; Wisniak, J.; Segura, H. Simultaneous prediction of the critical and sub-critical phase behavior in mixtures using equation of state I. Carbon dioxide-alkanols. *Chem. Eng. Sci.* **2001**, *56*, 6485–6510. [[CrossRef](#)]
36. Secuianu, C.; Feroiu, V.; Geană, D. Phase behavior for carbon dioxide + ethanol system: Experimental measurements and modeling with a cubic equation of state. *J. Supercrit. Fluids* **2008**, *47*, 109–116. [[CrossRef](#)]
37. Secuianu, C.; Feroiu, V.; Geană, D. Phase Behavior for the Carbon Dioxide + 2-Butanol System: Experimental Measurements and Modeling with Cubic Equations of State. *J. Chem. Eng. Data* **2009**, *54*, 1493–1499. [[CrossRef](#)]
38. Secuianu, C.; Feroiu, V.; Geană, D. High-pressure vapor-liquid equilibria in the system carbon dioxide and 2-propanol at temperatures from 293.25 K to 323.15 K. *J. Chem. Eng. Data* **2003**, *48*, 1384–1386. [[CrossRef](#)]
39. Sima, S.; Feroiu, V.; Geană, D. New High Pressure Vapor-Liquid Equilibrium and Density Predictions for the Carbon Dioxide plus Ethanol System. *J. Chem. Eng. Data* **2011**, *56*, 5052–5059. [[CrossRef](#)]
40. Guilbot, P.; Valtz, A.; Legendre, H.; Richon, D. Rapid on-line sampler-injector: A reliable tool for HT-HP sampling and online GC analysis. *Analisis* **2000**, *28*, 426–431. [[CrossRef](#)]
41. Geană, D.; Rus, L. Phase equilibria database and calculation program for pure components systems and mixtures. In Proceedings of the Romanian International Conference on Chemistry and Chemical Engineering (RICCCE XIV), Bucharest, Romania, 22–24 September 2005; Volume 2, pp. 170–178.
42. Cismondi, M.; Michelsen, M.L. Global Phase Equilibrium Calculations: Critical Lines, Critical End Points and Liquid–liquid–vapour Equilibrium in Binary Mixtures. *J. Supercrit. Fluids* **2007**, *39*, 287–295. [[CrossRef](#)]
43. Cismondi, M.; Michelsen, M. Automated Calculation of Complete Pxy and Txy Diagrams for Binary Systems. *Fluid Phase Equilib.* **2007**, *259*, 228–234. [[CrossRef](#)]
44. Cismondi, M.; Michelsen, M.L.; Zabaloy, M.S. Automated Generation of Phase Diagrams for Binary Systems with Azeotropic Behavior. *Ind. Eng. Chem. Res.* **2008**, *47*, 9728–9743. [[CrossRef](#)]
45. Heidemann, R.A.; Khalil, A.M. The calculation of critical points. *AIChE J.* **1980**, *26*, 769–779. [[CrossRef](#)]
46. Stockfleth, R.; Dohrn, R. An algorithm for calculating critical points in multicomponent mixtures which can easily be implemented in existing programs to calculate phase equilibria. *Fluid Phase Equilib.* **1998**, *145*, 43–52. [[CrossRef](#)]
47. Elizalde-Solis, O.; Galicia-Luna, L.A. Vapor-liquid equilibria and phase densities at saturation of carbon dioxide + 1-butanol and carbon dioxide + 2-butanol from 313 to 363. *Fluid Phase Equilib.* **2010**, *296*, 66–71. [[CrossRef](#)]
48. Stevens, R.M.M.; Shen, X.M.; de Loos, T.W.; de Swaan Arons, J. A new apparatus to measure the vapor-liquid equilibria of low-volatility compounds with near-critical carbon dioxide. Experimental and modelling results for carbon dioxide+n-butanol, +2-butanol, +2-butyl acetate and +vinyl acetate systems. *J. Supercrit. Fluids* **1997**, *11*, 1–14. [[CrossRef](#)]
49. Silva-Oliver, G.; Galicia-Luna, L.A. Vapor–liquid equilibria near critical point and critical points for the CO₂ + 1-butanol and CO₂ + 2-butanol systems at temperatures from 324 to 432 K. *Fluid Phase Equilib.* **2001**, *182*, 145–156. [[CrossRef](#)]
50. Ziegler, J.W.; Chester, T.L.; Innis, D.P.; Page, S.H.; Dorsey, J.G. Supercritical fluid flow injection method for mapping liquid–vapor critical loci of binary mixtures containing CO₂. In *Innovations in Supercritical Fluids. Science and Technology*; ACS Symposium Series; Hutchenson, E.K.H., Foster, N.R., Eds.; American Chemical Society: Washington, DC, USA, 1995; Volume 608, pp. 93–110. [[CrossRef](#)]
51. Yeo, S.-D.; Park, S.-J.; Kim, J.-W.; Kim, J.-C. Critical Properties of Carbon Dioxide + Methanol, + Ethanol, + 1-Propanol, and + 1-Butanol. *J. Chem. Eng. Data* **2000**, *45*, 932–935. [[CrossRef](#)]
52. Gurdial, G.S.; Foster, N.R.; Yun, S.L.J.; Tilly, K.D. Phase Behavior of Supercritical Fluid—Entrainer Systems. In *Supercritical Fluid Engineering Science. Fundamentals and Applications*; ACS Symposium Series; Kiran, E., Brennecke, J.F., Eds.; American Chemical Society: Washington, DC, USA, 1992; Volume 514, pp. 34–45. [[CrossRef](#)]
53. Sima, S.; Racoviță, R.C.; Dincă, C.; Feroiu, V.; Secuianu, C. Phase equilibria calculations for carbon dioxide + 2-propanol system. *U.P.B. Sci. Bull. Ser. B* **2017**, *79*, 11–24.
54. Reid, R.C.; Prausnitz, J.M.; Poling, B.E. *The Properties of Gases and Liquids*, 4th ed.; McGraw-Hill: New York, NY, USA, 1987.
55. Poling, B.E.; Prausnitz, J.M.; O’Connell, J.P. *The Properties of Gases and Liquids*, 5th ed.; McGraw-Hill Education: New York, NY, USA, 2001.

56. Design Institute for Physical Properties, Sponsored by AIChE. (2005; 2008; 2009; 2010; 2011; 2012; 2015; 2016; 2017; 2018; 2019; 2020). *DIPPR Project 801-Full Version*. Design Institute for Physical Property Research/AIChE. Available online: <https://app.knovel.com/hotlink/toc/id:kpDIPPRPF7/dippr-project-801-full/dippr-project-801-full> (accessed on 20 January 2022).
57. Jaubert, J.-N.; Le Guennec, Y.; Pina-Martinez, A.; Ramirez-Velez, N.; Lasala, S.; Schmid, B.; Nikolaidis, I.K.; Economou, I.G.; Privat, R. Benchmark Database Containing Binary-System-High-Quality-Certified Data for Cross-Comparing Thermodynamic Models and Assessing Their Accuracy. *Ind. Eng. Chem. Res.* **2020**, *59*, 14981–15027. [[CrossRef](#)]
58. Büchner, E.H. Liquid Carbonic Acid as a Solvent. *Z. Phys. Chem. Stoichiom. Verwandtschaftsl.* **1906**, *54*, 665–688. [[CrossRef](#)]